Momentum-transfer dependence of the Lyman-Birge-Hopfield and the K-shell preionization lines in the nitrogen molecule by means of high-energy electron-impact spectroscopy

Ronaldo S. Barbieri and R. A. Bonham
Department of Chemistry, Indiana University, Bloomington, Indiana 47405
(Received 18 November 1991)

The generalized-oscillator-strength (GOS) distribution for the Lyman-Birge-Hopfield (LBH) and the K-shell preionization lines in the nitrogen molecule, obtained with electron impact energies of 25–28 keV, are reported for the momentum-transfer range of 0.5–3.1 a.u. The results for the LBH were found to be in agreement with previously published low-energy experiments and also the most recent theoretical predictions. Possible reasons for problems encountered in previous high-energy electron spectroscopic experiments are discussed. The results for the preionization line confirm the measurements of Camilloni *et al.* [J. Phys. B **20**, 1839 (1987)] and agree with the theory presented in the following paper [Bielschowsky, Nascimento, and Hollauer, Phys. Rev. A **45**, 7942 (1992)]. The reliability of the results presented here can in part be judged by the quality of the optical-oscillator-strength distribution obtained by extrapolating the GOS to zero momentum transfer.

PACS number(s): 34.80.Gs, 34.50.Gb

I. INTRODUCTION

The relationship between the double differential cross section $d^2\sigma/d\Omega dE$ and the generalized oscillator strength (GOS) $df(K,E)/dE$ for molecular and atomic excitations, within the framework of the first Born approximation, is given approximately by [1]

$$\frac{d^2\sigma}{d\Omega dE}=(k_i/\{k_f(E)[K(E)]^2E\})\frac{df(K,E)}{dE}\ , \qquad (1)$$

where E is the energy loss, k_i and $k_f(E)$ are the initial and final momenta of the projectile electron, $K(E)$ is the momentum transfer, and Rydberg atomic units are used here and in the following. As it has been shown by Lassettre, Skeberle, and Dillon [2], in the limit as $K(E)$ approaches zero, the GOS converges to the optical oscillator strength (OOS), which can also be measured by photoabsorption methods. At small momentum transfer we can use the expansion [3]

$$\frac{df(K,E)}{dE}=f^{(0)}(E)+[K(E)]^2f^{(1)}(E)+[K(E)]^4f^{(2)}(E)+\cdots \qquad (2)$$

to extrapolate the GOS and to obtain the OOS $[f^{(0)}(E)]$. More can be extracted from the expansion given by Eq. (2) considering that the term $f^{(1)}(E)$ carries information on the probability for the excitation of quadrupole and octapole transitions in atoms and molecules [3,4].

The study of the GOS and cross sections of atmospheric gases is of importance in the understanding of several astrophysical, photochemical, and radiative processes. In particular, the dipole-forbidden quadrupole-allowed $X^1\Sigma_g^+\rightarrow a^1\Pi_g$ transition, best known as the Lyman-Birge-Hopfield (LBH) band, and the K-shell preionization line, near 401-eV energy loss, in N_2 have been the subject of previous studies.

The LBH band has been investigated by electron-impact spectroscopy at energies ranging form 300 to 35 000 eV [5–12], covering a range in the square of the momentum transfer K^2 up to 53 a.u. Good agreement is observed between the results provided by the lower impact energies up to 2000 eV, within their respective uncertainties, while the only high-energy results by Wong *et al.* [8] are higher by a factor of 1.2–1.3 over the whole K^2 range investigated. Discrepancies are also observed between theoretical studies of the LBH band in N_2. Szabo and Ostlund [13], using Slater-type orbitals in random-phase approximation and Tamm-Dancoff approximation, were not able to predict accurate values for the K^2 range below 1 a.u. Chung and Lin [14], working with Hartree-Fock (HF) wave functions in the Born-Ochkur-Bonham approximation, and the Tamm-Dancoff Hartree-Fock calculation by Greenwald and Langhoff [15] predicted the GOS distribution previously obtained with high-energy electrons [8]. However, the most recent theoretical values reported by Bielschowsky, Nascimento, and Hollauer [16], using both configuration-interaction (CI) and HF wave functions employing Gaussian-type orbitals, agree much better with the lower-energy experimental results at small and intermediate K^2 ranges. Hence a reinvestigation using high-energy electrons appears to be warranted.

The inner-shell excitation of atoms and molecules has been extensively investigated by energy-loss electron spectroscopy and photoabsorption techniques [17]. The absolute oscillator strength for the K-shell preionization peak $(^1\Sigma_g^+\rightarrow\Pi_{u,g})$ in N_2, obtained from experiments [18–23] at or near $K=0$, span the range from 0.12 to 0.23, with uncertainties no higher than 0.06, while theoretical predictions [24–30] are in the range from 0.13 up to 0.37. The biggest discrepancies are observed for those values obtained by photoabsorption: 0.12 and 0.23 [18,20]. No measurements of the GOS distribution for the N_2 preionization line have been performed for impact energies above 3400 eV.

In this work values of the GOS for the LBH and preionization bands in N_2, obtained by use of high-energy electron-impact spectroscopy, are reported. We have used the Bethe sum rule [3] for normalization of our results instead of normalizing them with respect to the elastic line, as usually done in low-energy experiments. The reliability of our results can be judged by comparing the OOS obtained by extrapolation of our GOS results with previously measured values.

II. EXPERIMENTAL PROCEDURES

The experimental setup and procedures have been described elsewhere [31]. Briefly, a 25–28-keV electron beam with a current of about 50 μA was arranged to cross an N_2 gas beam effusing out of a Pt nozzle of 150 μm diameter. Electron-energy-loss spectra, from 4 to 850 or 1000 eV, as a function of the scattering angle θ, were recorded by use of a Möllenstedt energy analyzer. The angular range covered was from 0.6° to 4.2° (momentum-transfer range of 0.5–3.1 a.u.), with an energy resolution of 2.0–4.0 eV, depending on the scattering angle. A relative GOS distribution was calculated as

$$\left[\frac{df(K(E),E)}{dE}\right]_{\text{rel}} = I_{\text{kin}}(\theta,E)I_{\text{expt}}(\theta,E)K_{\text{Kol}}(E)/F_{\text{ex}}(\theta,E) \quad (3)$$

with $I_{\text{exp}}(\theta,E)$ the detector dead-time-corrected relative experimental intensity, $I_{\text{kin}}(\theta,E)$ is a kinematic factor that includes relativistic correction for the incident electron, $F_{\text{ex}}(\theta,E)$ is an exchange scattering correction, and $K_{\text{Kol}}(E)$ is the Kollath correction due to the increase in the energy analyzer resolution as E increases. The expressions for k_i, $k_f(E)$, and $K(E)$ used in the calculation of the relative GOS were relativistic. For each relative GOS distribution a parametrized hydrogenic tail model was employed in order to estimate the GOS for energy-loss values above the energy of the last experimentally collected point. Our relative GOS distribution was then normalized by considering only the valence-shell block of each spectrum. In this first normalization procedure, which was based on the fact that $K(E)\approx\bar{K}$ with $\bar{K}$ the binary-encounter value given by $E_0\sin^2\theta$, where E_0 is the incident electron energy and θ is the scattering angle, the energy-loss range of the valence part of the spectrum was sum-rule normalized to 10. After constant angle-to-constant K corrections were applied to the GOS distribution [31] a second normalization was performed by use of the Bethe sum rule [3] $\int dE\, df(\bar{K},E)/dE = N$, with N being the number of electrons in the target ($N=14$ for the N_2 case).

III. RESULTS

A. The LBH band

A total of 25 data sets containing values of $df(K(E),E)/dE$ for the energy-loss range from 5.8 to 850 eV have been deposited with PAPS [32]. Although our data are not nearly as well resolved for the LBH band in N_2 as those of Wong *et al.* [8], we decided to estimate its GOS using an analytical procedure justifiable by the nonexistence of any prominent electronic spectral feature between the band itself and the elastic line. Integrated oscillator strengths for the LBH band in N_2 were then estimated by use of plots like the one shown in Fig. 1. The dashed line goes through the positive slope side of the LBH band, intercepting both the energy-loss axis and a vertical line at $E=9.35$ eV, which is the centroid of the band. In Fig. 1, b(eV) is the distance from the intercept on the E to the 9.35-eV vertical line and h(a.u.) is the height of the intersection point of the dashed slope line and the vertical line from the E scale. The GOS values for the LBH band were then estimated by use of the relation

$$\left[\frac{df(\bar{K},E)}{dE}\right]_{\text{LBH}} = b(\text{eV})h(\text{a.u.})/13.605\ \text{eV} . \quad (4)$$

The positive error in the above procedure was taken to be 15% of $[df(\bar{K},E)/dE]_{\text{LBH}}$, while the negative error was taken as $2b(\text{eV})[df/dE(7\ \text{eV})]/13.605$ eV. This last error estimate allows for the existence of a background as large as the GOS value at 7 eV.

In Table I and Fig. 2 our absolute GOS results for the LBH band in N_2 as a function of $\bar{K}^2$ are compared with those experimentally obtained with 1-keV incident electrons by Lucas and Souza [10,11], Fainelli *et al.* [12], and Wong *et al.* [8], where the latter were obtained with high-energy electrons (25–45 keV). The theoretical results from Bielschowsky, Nascimento, and Hollauer [16] obtained by use of CI double or CI double plus quadruple level of excitation, which of all published theoretical re-

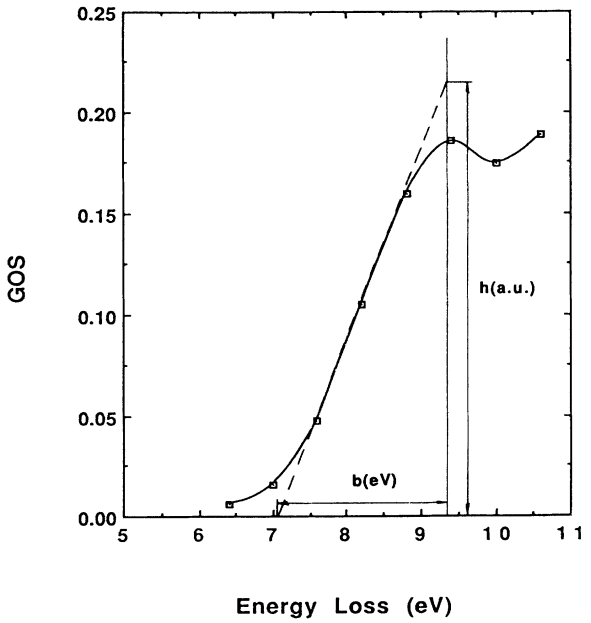

FIG. 1. Scheme used to calculate the integrated oscillator strength for the Lyman-Birge-Hopfield band in N_2. Actual GOS values in Rydberg atomic units (a.u.) at $\bar{K}=0.56$ are shown. The energy scale is given in eV.

TABLE I. GOS distribution for the LBH transition in N_2.

	Expt.				
K^2 (a.u.)	This work[a]	Fainelli *et al.*[b]	Lucas and Souza[c]	Wong *et al.*[d]	Theory[e]
0.065			0.013	0.014	
0.09		0.016(1)	0.017		0.013
0.20		0.026(2)	0.028		0.027
0.26	0.035(7)			0.041	
0.36		0.035(3)	0.039		
0.38	0.038(08)				
0.49	0.042(08)			0.058	0.040
0.56		0.041(3)	0.043		
0.68	0.048(09)			0.063	
0.80			0.045	0.064	0.049
0.81		0.043(3)			
0.86			0.046		
0.90	0.048(09)			0.063	0.049
1.09			0.041		
1.10		0.037(3)			
1.22	0.042(08)			0.056	
1.35	0.039(08)				
1.39	0.042(08)				0.041
1.43			0.037		
1.44		0.033(3)		0.051	
1.48	0.040(08)				
1.66	0.033(07)			0.045	
1.80			0.027		0.035
1.82		0.031(3)			
1.89	0.031(06)			0.040	
2.15	0.023(05)			0.035	
2.24		0.025(2)			
2.47	0.021(04)				
2.67	0.023(05)			0.028	
2.69			0.023		0.021
2.79			0.019		
2.91	0.018(04)				
3.18	0.018(04)			0.024	
3.23		0.018(2)			
3.70	0.015(03)			0.020	0.011
4.38	0.010(02)			0.017	
4.48			0.015		
5.02	0.013(03)	0.010(1)		0.014	
5.91	0.0088(18)			0.011	
6.48	0.0065(13)			0.0093	
6.97	0.0088(18)				
7.99			0.011	0.0064	
8.91		0.0049(4)			
9.68	0.0065(13)			0.0042	
19.8		0.0038(4)			
34.5		0.0018(2)			
52.7		0.0009(1)			

[a]Numbers in parentheses are the positive uncertainties for the last two digits. Negative uncertainties are larger.

[b]From Ref. [12]. Numbers in parentheses are the uncertainties for the last digit.

[c]From Refs. [10] and [11]. The error estimate is 10%.

[d]Values estimated from the smoothed experimental curve in Ref. [8]. No uncertainty was given in this reference.

[e]From Bielschowsky, Nascimento, and Hollauer [16].

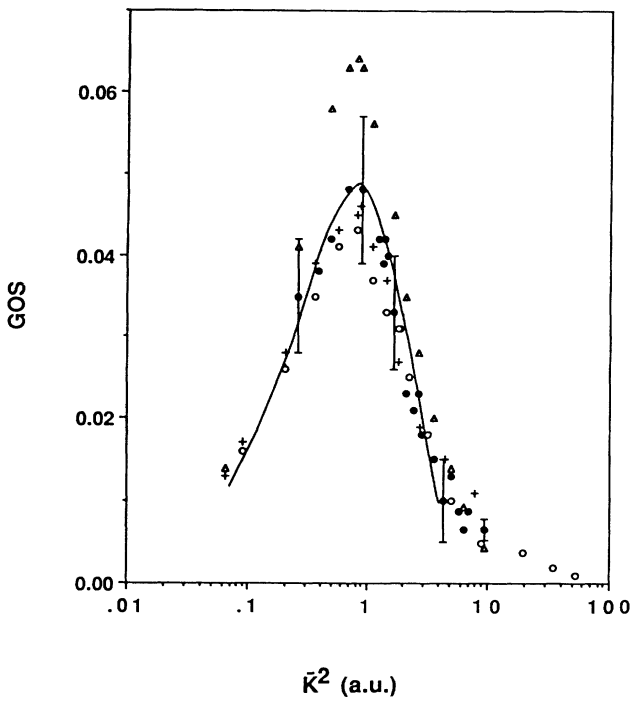

FIG. 2. The GOS distribution for the Lyman-Birge-Hopfield band in N_2 plotted in Rydberg a.u. on both axes. Experiments: triangles, Wong *et al.* [8]; crosses, Lucas and Souza [10,11]; open circles, Fainelli *et al.* [12]; closed circles, this work. Theory (solid line) is from Bielschowsky, Nascimento, and Hollauer [16].

sults agree best with the experiments, are also included in Fig. 2. The experimental results of Lassettre and coworkers [5,7], at 300, 400, and 500 eV, and Oda and Osawa [9], at 500, 700, 1000, and 2000 eV, are not shown here since they agree with those by Lucas and Souza [10,11] and Fainelli *et al.* [12].

As can be seen in Fig. 2 our results are in very good agreement with those by Lucas and Souza [10,11] and Fainelli *et al.* [12]. The work reported by Wong *et al.* [8] appears to be systematically about 20–30% too high compared to the other experimental results in Fig. 2 in spite of the fact that the energy resolution reported by them is far superior to that employed here. This leads us to believe that a problem could have occurred in the normalization of the work in Ref. [8] since the strongest point in the present work is the determination of the absolute scale. In Ref. [8] the data were placed on an absolute scale by matching a high-resolution (1.5 eV) spectral scan (5–30 eV) to a complete scan (5–1000 eV) at lower resolution (3 eV), sum-role normalized to an absolute scale, in the energy range from 20 to 30 eV. The question immediately arises as to whether this procedure was justified, which we show from the analysis presented below that it may not be.

We wish to consider what happens when relatively smooth experimental data is convoluted with an asymmetrical energy resolution function. We assume that the GOS is representable over the region of interest as

$$\frac{df(\bar{K},E)}{dE}=f^{(0)}(E_0)+f^{(1)}(E_0)(E-E_0)+f^{(2)}(E_0)(E-E_0)^2+\cdots \tag{5}$$

and that the experimentally observed GOS is given by

$$\left\langle\frac{df(\bar{K}E_0)}{dE}\right\rangle=(1/2\pi\sigma^2)^{1/2}\times\int_{-\infty}^{\infty}dE\left[[1+C_0(E-E_0)]\times\exp[-(E-E_0)^2/2\sigma^2]\times\frac{df(\bar{K},E)}{dE}\right], \tag{6}$$

where it has been assumed that σ, approximately one-half the energy resolution reckoned as the full width at half the maximum height (FWHM) of the elastic line, is small compared to the energy loss width of the region of interest. If the expansion in (5) is substituted into Eq. (6) and the integrations carried out it is possible to write Eq. (6) as

$$\left\langle\frac{df(\bar{K},E_0)}{dE}\right\rangle=f^{(0)}(\bar{K},E_0)+\langle(E-E_0)\rangle f^{(1)}(\bar{K},E_0)+\langle(E-E_0)^2\rangle f^{(2)}(\bar{K},E_0)/2+\langle(E-E_0)^3\rangle f^{(3)}(\bar{K},E_0)/6\ , \tag{7}$$

where

$$f^{(n)}(\bar{K},E_0)=\left[\frac{d}{dE}\right]^n\frac{df(\bar{K},E)}{dE}\bigg|_{E=E_0} \tag{8}$$

and

$$\langle(E-E_0)^n\rangle=(1/2\pi\sigma^2)^{1/2}\times\int_{-\infty}^{\infty}dE(E-E_0)^n[1+C_0(E-E_0)]\times\exp[-(E-E_0)^2/2\sigma^2]\ . \tag{9}$$

The results for the first three moments as defined in Eq. (9) are given by

$$\langle(E-E_0)\rangle=\sigma y\ , \tag{10}$$

$$\langle(E-E_0)^2\rangle=\sigma^2\ , \tag{11}$$

and

$$\langle(E-E_0)^3\rangle=3\sigma^3 y\ , \tag{12}$$

where y is a dimensionless parameter given by σC_0. Equation (7) tells us that, as long as the GOS is a straight line with zero slope across the width of the energy-resolution function, the experimental convolution has no effect on the GOS. On the other hand, if the GOS possesses a nonzero slope and or curvature in the region where a match is made, then the exact value of the experimentally convoluted GOS will depend on the slope and higher derivatives of the GOS with respect to energy loss and also on the energy resolution. For the case in question we can write the absolute (abs) intensity of the high-resolution part of the spectrum at an energy loss E in terms of the measured relative (rel) intensity as

$$\left\langle \frac{df(\bar{K},E}{dE} \right\rangle_{\text{abs}} = \left\langle \frac{df(\bar{K}E)}{dE} \right\rangle_{\text{rel}} \left[\left\langle \frac{df(\bar{K},E_0)}{dE} \right\rangle_{\text{abs}} \Big/ \left\langle \frac{df(\bar{K},E_0)}{dE} \right\rangle_{\text{rel}} \right]$$

$$= \left\langle \frac{df(\bar{K},E)}{dE} \right\rangle_{\text{rel}} A_0(\{1+\langle E-E_0\rangle_l f^{(1)}(\bar{K},E_0)/f^{(0)}(\bar{K},E_0)$$

$$+\langle (E-E_0)^2\rangle_l f^{(2)}(\bar{K},E_0)/[2f^{(0)}(\bar{K},E_0)]\cdots\}$$

$$\times\{1+\langle (E-E_0)\rangle_h f^{(1)}(\bar{K},E_0)/f^{(0)}(\bar{K},E_0)$$

$$+\langle (E-E_0)^2\rangle_h f^{(2)}(\bar{K},E_0)/[2f^{(0)}(\bar{K},E_0)]\cdots\}^{-1}) , \tag{13}$$

where l refers to the lower-resolution spectrum, h refers to the higher resolution spectrum, E_0 is the energy loss at which the two spectra are normalized to each other, and A_0 is the ratio of the sum-rule normalized low resolution intensity to the high-resolution un-normalized intensity at the energy-loss match point. The assumption has been made that the resolution correction does not make an important contribution to the sum rule. That this assumption is warranted has been justified in detail elsewhere [33].

Unfortunately the original data from Ref. [8] are not available for analysis, but we can make use of the present data to see if the slope and curvature in the matching region could possibly explain the previous results. The quantities which we normally use to characterize the elastic line in the spectrum are the center of gravity of the line $\langle E\rangle$, the standard deviation of the line $[\langle E^2\rangle-\langle E\rangle^2]^{1/2}$, and the skewness $[\langle E^3\rangle-\langle E\rangle^3]/[\langle E^2\rangle-\langle E\rangle^2]^{3/2}$. For the assumed analytic shape of the experimental resolution function these quantities are given as

$$\langle E\rangle = E_0+\sigma y , \tag{14}$$

$$[\langle E^2\rangle-\langle E\rangle^2] = \sigma^2(1-y^2) , \tag{15}$$

and

$$[\langle E^3\rangle-\langle E\rangle^3]/[\langle E^2\rangle-\langle E\rangle^2]^{3/2} = 2y^3/(1-y^2)^{3/2} . \tag{16}$$

For the present data, using a scattering angle of 3°, we have found that

$$f^{(1)}(\bar{K},E_0)/f^{(0)}(\bar{K},E_0) = 1.4\pm0.3$$

and

$$f^{(2)}(\bar{K},E_0)/[2f^{(0)}(\bar{K},E_0)] = 0.9\pm0.4$$

for energy losses between 20 and 30 eV. For the 25 data sets in the present experiment the standard deviation of the elastic line ranged from 1.1 to 2.0 eV with an average value of 1.5 eV, while the skewness ranged from −0.01 to 0.19 with an average value of 0.06. If we take the maximum of the observed values in order to establish an order-of-magnitude estimate of the possible error in the normalization, we obtain a correction of 0.88, which is in the right direction and accounts for 60% of the difference between the results obtained in Ref. [8] and this work. As an added check we calculated the center of gravity of the elastic line $\langle E\rangle$ and the position of the maximum of the elastic line E_m for which the difference is given for our assumed energy resolution function as

$$\langle E\rangle - E_m = \sigma y^3(1-2y^2+y^4+\cdots) . \tag{17}$$

For the parameters used above Eq. (17) predicts a value of 0.1 eV. The observed values for six elastic lines at scattering angles between 0.6° and 3.5° ranged from −0.37 to +0.20 eV with an average value of +0.03 eV. We conclude from this analysis that the problem with the results of Ref. [8] could very well have been due to lack of consideration of the effects of the slope and curvature of the GOS on the convolution of the data with the resolution function of the energy analyzer.

B. The preionization line

One of the main features of the K-shell spectra of N_2 is the $^1\Sigma_g^+ \rightarrow {}^1\Pi_{u,g}$ transition at $E=401.1$ eV. It is due to the excitation of an inner-shell electron in N_2 to the antibonding orbital $2p\pi_g$, the first unfilled molecular orbital of the molecule. Its vibrational structure has been investigated by King, Read, and Tronc [34] by inelastic scattering of 1.5-keV electrons in the forward direction with 75-meV energy resolution. Spin-forbidden transitions from the ground state to the triplet $^3\Pi_{u,g}$ state in N_2 at $E=400.2$ eV have been reported by Shaw *et al.* [35], although contributions form these transitions would not be expected to be observable at our incident energies. Other important features in the inner-shell spectrum of N_2 include the excitation of a $1s$ electron to discrete Rydberg orbitals [36–38] in the energy-loss range from 406 to 410 eV. Above the K edge there are also two doubly excited states at 414.0 and 415.0 eV, a shape resonance peaking near 419 eV, and a shake-up continua [36,37]. Moreover, dissociation of N_2 associated with K-shell excitation has been extensively investigated [39].

Although the OOS for the preionization peak in N_2 has been determined in several experiments [18–23], only the experiment by Camilloni *et al.* [22,23] with incident electrons of 1400 and 3400 eV has reported the GOS distribution for the peak area as a function of the momentum transfer. They achieved an energy resolution (FWHM) of 0.7 and 1.2 eV, respectively, at these energies. Their absolute values for the differential cross sections of the peak were normalized with respect to the absolute differential elastic cross section for N_2 from Jansen *et al.* [40].

Our results for the GOS of the preionization resonance

TABLE II. GOS distribution for the preionization peak in N_2.

	Expt.		Theory	
K^2 (a.u.)	This work[a]	Camilloni *et al.* [22][b]	Bielschowsky, Nascimento, and Hollauer [30]	Rescigno and Orel [27]
0.01		0.203	0.20	0.236
0.1		0.201	0.20	
0.25	0.182	0.197		
0.377	0.179	0.194		
0.5			0.20	
0.624	0.171	0.188		
0.677	0.179			
0.899	0.177	0.182		
1.0		0.180	0.19	0.214
1.1	0.175			
1.35	0.183	0.173		
1.39	0.182			
1.48	0.190			
1.66	0.175	0.167		
1.89	0.179			
2.0			0.18	0.196
2.15	0.174	0.157		
2.47	0.161			
2.67	0.180	0.148		
2.91	0.165			0.182
3.0		0.143	0.17	
3.18	0.159			
4.0		0.129	0.16	0.166
4.38	0.161	0.123		
5.0	0.157	0.116	0.15	0.154
5.91	0.144			
6.0		0.105	0.14	0.142
6.48	0.145			
6.97	0.135	0.096	0.13	0.127
8.0			0.12	
9.68	0.118			
10.0			0.11	
11.0			0.057	
12.0			0.032	
13.0			0.020	

[a]Results obtained by numerical integration (see text). Error estimated to be 11%.
[b]Estimated error of 8%.

peak in the nitrogen molecule are presented in Table II and Fig. 3. Our results are compared to the fit to the experimental data of Camilloni *et al.* [23] and to the theoretical results by Bielschowsky, Nascimento, and Hollauer [30], obtained by use of a generalized multistructural (GMS) wave function in a nonorthogonal CI approach, and by Rescigno and Orel [27]. Both works have calculated the GOS as the sum of the $^1\Pi_u$ and $^1\Pi_g$ contributions. Results from Ref. [23] were obtained by use of Eq. (2) with values reported for the coefficients up to $f^{(5)}$. Our results were obtained by numerically integrating the GOS distribution, at each K value, in the energy loss interval from 394 to 406 eV. These results were checked by integrating a Gaussian curve fitted to the GOS in the same E range. Although the Gaussian curve was not skewed to higher energy loss, as expected due to the vibrational structure of the preionization peak [34], the area obtained from the fit agreed with the values estimated numerically to 11%. The statistical error from the total number of counts accumulated at each scattering angle in the 400-eV energy loss peak was about 3%.

Our GOS results for the preionization line in N_2 agree with those by Camilloni *et al.* [23] within experimental error in the K^2 range up to 3 a.u., although our values are somewhat lower for $K^2<0.5$ a.u. In the optical limit very good agreement is observed between the experimental results in Ref. [23] and the GMS model calculations from Bielschowsky, Nascimento, and Hollauer [30]. However, this is not the case as K^2 increases since the theory seems to agree much better with our values than those by Camilloni *et al.* [23] for $K^2>2$. Good agreement is also observed between our results and the values from Rescigno and Orel [27] (not shown in Fig. 3) for $K^2>2$ a.u. These authors found, through CI calcula-

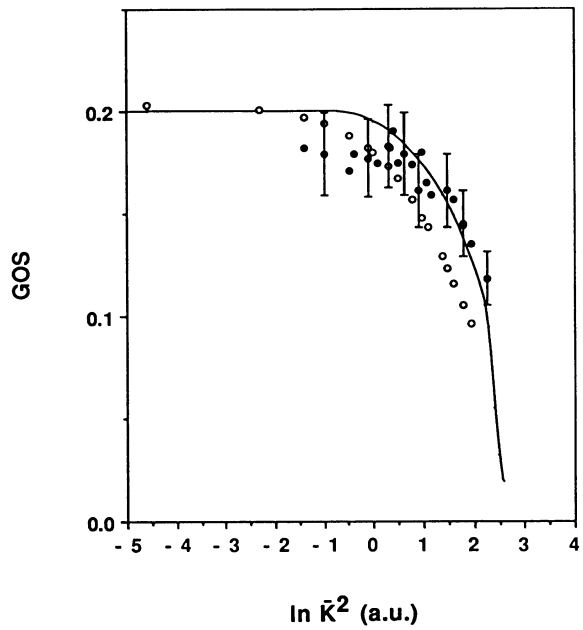

FIG. 3. The GOS distribution for the preionization line in N_2 plotted in Rydberg a.u. on both axes. Experiments: open circles, Camilloni *et al.*, [23]; closed circles, this work. Theory (solid line) is from Bielschowsky, Nascimento, and Hollauer [30] based on the GMS model.

tions, a splitting of the states $^1\Pi_u$ and $^1\Pi_g$ of 60 meV [27], while Butscher, Buenker, and Peyerimhoff obtained a value of 220 meV [41]. Due to the energy resolution of our experiment and that employed by Camilloni *et al.* [23] these two states were not resolved. For this reason, the theoretical values in Table II represent the sum of the GOS's for the $^1\Pi_u$ and $^1\Pi_g$ states.

C. The OOS distribution

In order to verify the reliability of the Bethe surface we have obtained for N_2 [31] and employed here we have determined the photoabsorption distribution. A total of 159 $f^{(0)}(E)$ points were generated in the energy-loss range from 6.4 to 850 eV by use of Eq. (2). At each

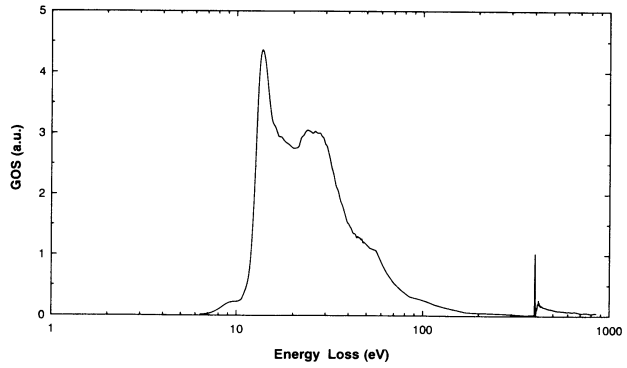

FIG. 4. The OOS distribution for the N_2 molecule. The horizontal logarithmic scale is the energy loss given in eV and the vertical scale is the absolute OOS given in Rydberg a.u.

energy-loss value, 10 experimental data points of the GOS in the $\bar{K}^2$ range from 0.25 to 1.7 a.u. were least-squares fitted with first-, second-, and third-order polynomials. In Table III, our results for $f^{(0)}(E)$ for the nitrogen molecule are presented and compared to the experimental results from Wight, van der Wiel, and Brion [42], Kay, van der Leeuw, and van der Wiel [19], and Cole and Dexter [43]. The overall shape of the OOS is displayed in Fig. 4.

The orders of the polynomials employed to obtain our values are shown for each energy loss value in the column on the far right in Table III. The tabulated uncertainties $\Delta f^{(0)}(E)$ are either the fitting uncertainties or the difference between the indicated $f^{(0)}(E)$ and the nearest $f^{(0)}(E)$ value obtained by a polynomial fitting of a different order, whichever is larger. Values in parentheses represent the fitting uncertainties. The $f^{(0)}(E)$ values for the valence-shell block, up to 390 eV, in Table III are those with the lowest fitting uncertainties compared to those from other fitting orders. For the K shell, however, we have decided to use only second-order results, although those obtained by a linear fit usually had lower fitting uncertainties. The justification is that after adding the missing tail to the $f^{(0)}(E)$ distribution given by Table III, through a hydrogenic model described in detail in Ref. [31], the total area of the optical distribution was 14.1 ± 0.7. If only first-order values of $f^{(0)}(E)$ are employed for the K shell, the Bethe sum rule decreases to 13.2 ± 0.5. It is also worth mentioning that the OOS values for the preionization peak obtained by numerically integrating the first-, second-, and third-order $f^{(0)}(E)$ distributions from 396.4 to 403.6 eV are 0.17, 0.19, and 0.25, respectively. The oscillator strength value obtained by extrapolating the second-order fit of the GOS distributions in Fig. 3 to $K=0$ is 0.18 ± 0.02. In Table IV $f^{(0)}(E)$ results for the preionization transition in N_2 are compared with other experimental and theoretical values available in the literature.

As seen from Table III good agreement is observed between our OOS results and those experimentally obtained by Wight, van der Wiel, and Brion [42] in the energy-loss range of 10–70 eV, which they have investigated by use of 8-keV electrons with a resolution of 0.5-eV FWHM. Their relative OOS values were obtained by extrapolating to $K=0$ their energy-loss spectra recorded at 0° and 0.6° by use of a two-term expansion at each energy loss. Their results were placed on an absolute scale by normalization at 32 eV with the absorption data by Samson and Cairns [44].

The photoabsorption results from Cole and Dexter [43] in Table III were obtained with synchrotron radiation for the energy-loss range of 36–248 eV. From 36 to 130 eV, their results are also in good agreement with our work. Above 140 eV their results are somewhat lower, although this does not seem to change the sum rule for the N_2 valence shell. In order to verify such a trend the function AE^{-B} was least-squares fitted to the OOS distribution form this work and also to the OOS data from Cole and Dexter [43] in the energy range from 115 to 248 eV. The values of A and B obtained from each fit were then used to estimate the missing area of the corresponding

TABLE III. Optical oscillator-strength distribution for N_2.

	This work			Wight, van der Wiel, and Brion[b]	Cole and Dexter[c]
E (eV)	$f^{(0)}(E)$	$\Delta f^{(0)}(E)$[a]	order	$f^{(0)}(E)$	$f^{(0)}(E)$
6.4	0.0159	(0.0100)	1		
7.0	0.0265	(0.0110)	1		
7.6	0.0635	0.0389	1		
8.2	0.121	0.042	1		
8.8	0.186	0.046	1		
9.4	0.220	0.052	1		
10.0	0.227	0.071	1		
10.6	0.259	0.082	1		
11.2	0.433	(0.038)	1		
11.8	0.843	0.197	1		
12.4	2.08	0.37	2		
13.0	3.74	0.67	3		
13.6	4.36	0.75	3		
14.2	4.15	0.56	3		
14.8	3.62	0.33	3		
15.4	3.21	0.17	3		
16.0	3.10	0.14	3		
16.6	2.96	0.13	2		
17.2	2.94	0.12	2		
17.8	2.88	0.06	2		
18.4	2.84	(0.04)	2		
19.0	2.81	(0.04)	2	2.95	
19.6	2.77	(0.05)	2		
20.2	2.75	(0.04)	2		
20.8	2.76	0.07	2		
21.4	2.79	0.07	2		
22.0	2.92	(0.04)	2	2.82	
22.6	2.96	(0.05)	2		
23.2	3.02	(0.05)	2		
23.8	3.05	0.06	2		
24.4	3.04	0.10	2		
25.0	3.02	0.08	2	2.88	
25.6	3.00	(0.08)	2		
26.2	3.03	(0.08)	2		
26.8	3.01	(0.08)	2		
27.4	3.00	0.17	2		
28.0	3.00	0.15	2	2.79	
28.6	2.95	0.18	2		
29.2	2.92	0.21	2		
29.8	2.83	0.17	2		
30.4	2.79	0.19	2		
31.0	2.69	0.21	2	2.44	
31.6	2.59	0.20	2		
32.2	2.46	(0.08)	2		
32.8	2.37	0.17	2		
33.4	2.27	0.17	2		
34.0	2.15	0.22	2	2.03	
34.6	2.09	0.21	2		
35.2	2.03	0.16	2		
35.8	1.93	0.14	2		
36.4	1.86	0.11	2		1.72
37.0	1.81	0.13	2	1.76	
37.6	1.74	(0.07)	2		1.68
38.2	1.67	0.12	2		
38.8	1.59	(0.06)	2		1.47
39.4	1.53	0.06	2		
40.0	1.51	0.07	2	1.52	1.39
40.6	1.47	0.08	2		

TABLE III. (*Continued*).

	This work			Wight, van der Wiel, and Brion[b]	Cole and Dexter[c]
E (eV)	$f^{(0)}(E)$	$\Delta f^{(0)}(E)$[a]	order	$f^{(0)}(E)$	$f^{(0)}(E)$
41.2	1.44	0.08	2		1.33
41.8	1.39	(0.06)	2		
42.4	1.35	(0.06)	2		
42.8					1.30
43.0	1.35	(0.05)	2	1.41	
43.6	1.33	(0.05)	2		
44.2	1.28	(0.05)	2		1.27
44.8	1.30	(0.05)	2		
45.4	1.28	(0.05)	2		
46.0	1.28	0.06	2	1.35	1.24
46.6	1.25	(0.05)	2		
47.2	1.26	(0.05)	2		
47.8	1.20	(0.05)	2		1.20
48.4	1.21	(0.04)	2		
49.6					1.17
52.0	1.11	(0.04)	2	1.16	1.07
53.9					1.00
56.2	1.07	0.15	1	0.982	
59.1					0.793
61.0	0.828	0.077	1	0.789	
62.0					0.706
64.0	0.706	0.023	1	0.721	
65.3					0.682
68.9				0.646	0.545
70.0	0.534	0.028	1		
72.6					0.483
76.6	0.416	0.038	1		
77.5					0.415
82.7					0.372
85.0	0.309	0.015	1		
				Kay, van der Leeuw, and van der Wiel[d] $f^{(0)}(E)$	
100.0	0.252	0.025	2	0.27	
115.0	0.182	0.017	2	0.16	
124.0					0.138
130.0	0.137	0.013	2	0.14	
137.8					0.105
145.9					0.0830
150.4	0.0961	(0.0074)	2	0.10	
155.0					0.0793
165.3					0.0682
170.2	0.0587	0.0171	1	0.075	
177.1					0.0570
190.0	0.0505	0.0215	1	0.054	
206.7					0.0397
210.4	0.0477	0.0121	1	0.042	
225.5					0.0310
230.2	0.0436	0.0088	1	0.034	
248.0					0.0223
250.0	0.0393	0.0076	1	0.029	
270.4	0.0350	(0.0066)	1		
290.2	0.0304	(0.0062)	1		
310.0	0.0251	(0.0058)	1	0.018	
330.0	0.0206	(0.0049)	1	0.015	
360.4	0.0132	0.0037	1	0.012	
390.4	0.0168	0.0073	2		
391.0	0.0051	(0.0030)	2		

TABLE III. (*Continued*).

	This work			Wight, van der Wiel, and Brion[b]	Cole and Dexter[c]
E (eV)	$f^{(0)}(E)$	$\Delta f^{(0)}(E)$[a]	order	$f^{(0)}(E)$	$f^{(0)}(E)$
391.6	0.0138	0.0040	2		
392.2	0.0127	(0.0097)	2		
392.8	0.0136	0.0084	2		
393.4	0.0142	0.0037	2		
394.0	0.0141	(0.0031)	2		
394.6	0.0153	0.0071	2		
395.2	0.0093	(0.0056)	2		
395.8	0.0064	(0.0146)	2		
396.4	0.0	(0.0235)	2		
397.0	0.0	(0.0429)	2		
397.6	0.0054	(0.1570)	2		
398.2	0.116	(0.238)	2		
398.8	0.365	(0.328)	2		
399.4	0.734	(0.369)	2	0.21	
400.0	1.00	(0.30)	2	0.94	
400.6	0.978	0.237	2	1.6	
401.2	0.669	(0.312)	2	1.2	
401.8	0.328	(0.314)	2	0.51	
402.4	0.0853	(0.3040)	2	0.18	
403.0	0.0		2	0.051	
403.6	0.0		2		
404.2	0.0		2		
404.8	0.0197	(0.0758)	2		
405.4	0.0490	(0.0271)	2		
406.0	0.0693	0.0036	2	0.073	
407.2	0.0949	0.0432	2		
408.4	0.102	0.0084	2		
409.6	0.133	0.017	2		
410.8	0.124	(0.014)	2	0.15	
412.0	0.162	0.033	2	0.15	
413.2	0.190	(0.030)	2	0.18	
414.4	0.197	0.026	2	0.22	
415.6	0.196	(0.013)	2	0.23	
416.8	0.201	0.017	2	0.23	
418.0	0.238	(0.018)	2	0.25	
419.2	0.246	(0.021)	2	0.27	
420.4	0.192	(0.025)	2	0.26	
421.6	0.211	0.035	2	0.25	
422.8	0.203	0.034	2	0.23	
424.0	0.174	(0.022)	2	0.22	
425.2	0.189	0.034	2	0.22	
426.4	0.170	0.028	2	0.21	
427.6	0.171	(0.020)	2		
428.8	0.163	(0.014)	2		
430.0	0.169	0.018	2		
436.0	0.161	0.018	2		
443.2	0.142	0.017	2		
450.4	0.140	(0.011)	2		
470.2	0.120	(0.010)	2		
490.0	0.111	0.014	2		
510.4	0.0946	0.0185	2	0.12	
530.2	0.0864	0.0183	2	0.10	
550.0	0.0821	0.0212	2	0.086	
570.4	0.0778	0.0222	2	0.082	
590.2	0.0726	0.0156	2	0.076	
610.0	0.0733	0.0129	2	0.068	
630.4	0.0650	0.0122	2		
650.2	0.0720	0.0221	2		

TABLE III. (*Continued*).

	This work			Wight, van der Wiel, and Brion[b]	Cole and Dexter[c]
E (eV)	$f^{(0)}(E)$	$\Delta f^{(0)}(E)$[a]	order	$f^{(0)}(E)$	$f^{(0)}(E)$
680.2	0.0581	0.0063	2		
710.2	0.0488	0.0126	2		
740.2	0.0530	(0.0035)	2		
770.2	0.0482	0.0059	2		
800.2	0.0386	0.0020	2		
825.4	0.0455	0.0127	2		
850.0	0.0443	0.0184	2		

[a]The error in $f_p^{(0)}(E)$ where p signifies the order of the fit is given by the larger of $|f_p^{(0)}(E)-f_{p\pm1}^{(0)}|$ or $\Delta f_p^{(0)}(E)$ from the least-squares fit. The latter are designated by the use of parentheses.
[b]Values from Ref. [42]. The maximum error is 6%.
[c]Values from Ref. [43]. Values have an absolute accuracy of 10%.
[d]Estimated from Ref. [19]. The error estimate is below 5%.

valence-shell OOS distribution by analytical integration. The contribution of our OOS distribution in the energy loss range from 6.4 to 115 eV was used in both cases because Cole and Dexter [43] have no data available for $E<36$ eV. The valence-shell sum rules for N_2 were found to be 10.2 ± 0.8 in our case, and 9.8 ± 0.9 when Cole and Dexter's [43] results are employed.

The results attributed to Kay, van der Leeuw, and van der Wiel [19] in Table III for the OOS near the K edge in N_2 have been estimated from Fig. 2 in Ref. [19]. These authors have also employed energy-loss spectroscopy, in the energy-loss range of 40–600 eV, with 8-keV impact electrons in the forward direction. Their results for the lowest energy portion were not available. Their absolute oscillator strengths in the energy loss interval from 40 to 60 eV are in excellent agreement with Wight, van der Wiel, and Brion [42], as claimed, and so with ours. Above 60 eV, except in the region of the preionization line, the OOS values of Kay, van der Leeuw, and van der Wiel [19] are also in good agreement with our corresponding results, within the tabulated uncertainties, as well as with the atomic calculations (not shown) of McGuire [45] and Veigel [46] for atomic nitrogen times a factor of 2. Although our optical preionization peak is broader (around 2.2-eV FWHM) than the peak reported by Kay, van der Leeuw, and van der Wiel [19] (around 1.5-eV FWHM), our integrated oscillator strength of 0.18 ± 0.02 agrees fairly well with their value of 0.195 ± 0.020 at $K=0.61$ a.u. (see Table IV). For the shape resonance in the K continuum in N_2, characterized by a broad peak at 419 eV, the agreement between the results from this work and from Ref. [19] is also good. In both cases the resonance maximum is around 419 eV, as previously predicted by others through energy loss spec-

TABLE IV. Absolute OOS for the preionization line in N_2.

Method	$f^{(0)}$
By optical absorption	
Wuilleumier and Krause [18]	0.12 ± 0.05[a]
Bianconi *et al.* [20]	0.23 ± 0.06[a]
By the electron energy loss technique	
Kay, van der Leeuw, and van der Wiel [19]	0.195 ± 0.02[b]
Oda, Nishimura, and Osawa [21]	0.14 ± 0.01[c]
Camilloni *et al.* [23]	0.20 ± 0.02[d]
This work	0.18 ± 0.02[d]
Theory	
Dehmer and Dill [24]	0.23
Rescigno and Langhoff [25]	0.257
Iwata, Kosugi, and Nomura [26]	0.368
Arneberg *et al.* [28]	0.13
Rescigno and Orel [27]	0.236
Barth and Schimer [29]	0.20
Bielschowsky, Nascimento, and Hollauer [30]	0.20

[a]Results obtained from x-ray absorption spectroscopy.
[b]Value for $K=0.61$ a.u.
[c]Value for $K=1.85$ a.u.
[d]Extrapolated values by use of Eq. (2).

tra [37] or by photoabsorption [47]. Dehmer and Dill [24] have made calculations for the shape resonances in N_2 based on a multiple-scattering model which resulted in a narrower and taller peak shifted by 3 eV to higher-energy loss. Stiltjes-Tchebycheff calculations in the static-exchange approximation by Rescigno and Langhoff [25] seem to give a better description of the intensity of the shape resonances in N_2, although their maximum is shifted down to 416 eV.

IV. CONCLUSIONS

The GOS distributions for the LBH and preionization transitions in N_2 as well as its photoabsorption spectrum have been investigated in this work by high-energy (25–28 keV) electron-impact spectroscopy. The absolute Bethe surface employed here [31] was obtained within the framework of the Bethe-Born approximation [3]. Normalization of our results was based on the Bethe sum rule [3].

The results obtained agree with those given by Stefani and co-workers (see Refs. [12], [22], and [23]), also obtained by energy-loss spectroscopy with impact energies up to 3.4 keV, and with the theoretical predictions by Bielschowsky, Nascimento, and Hollauer [16,30]. Our photoabsorption distribution, $f^{(0)}(E)$ vs E, for N_2 is the most reliable extrapolation of a Bethe sum-rule normalized GOS to zero momentum transfer so far reported. No further normalization was performed after the extrapolation. Our OOS distribution satisfies the Thomas-Reiche-Kuhn sum rule [3] and agrees with those previously obtained by electron-energy loss [19,42] and by photoabsorption [43,44]. Predictions made by Dehmer and Dill [24] for the shape resonances in the N_2 K continuum are in semiquantitative agreement with the results from this work and Kay, van der Leeuw, and van der Wiel [19].

ACKNOWLEDGMENTS

The authors acknowledge the National Science Foundation for Grant No. PHY-8913096. R.S.B. wishes to thank the CNPq (Brazil) for their support of this work. We are also grateful to Dr. Carlos E. Bielschowsky for sending us the results for the preionization line in advance of publication.

[1] H. Bethe, Ann. Phys. (Leipzig) **5**, 325 (1930).
[2] E. N. Lassettre, A. Skeberle, and M. A. Dillon, J. Chem. Phys. **50**, 1829 (1969).
[3] M. Inokuti, Rev. Mod. Phys. **43**, 297 (1971).
[4] R. A. Bonham, M. Inokuti, and R. S. Barbieri (unpublished).
[5] E. N. Lassettre and M. E. Krasnow, J. Chem. Phys. **40**, 1248 (1964).
[6] E. N. Lassettre, A. Skeberle, M. A. Dillon, and K. J. Ross, J. Chem. Phys. **48**, 5066 (1968).
[7] A. Skeberle and E. N. Lassettre, J. Chem. Phys. **53**, 3806 (1970).
[8] T. C. Wong, J S. Lee, H. F. Wellenstein, and R. A. Bonham, J. Chem. Phys. **63**, 1538 (1975).
[9] N. Oda and T. Osawa, J. Phys. B **14**, L563 (1981).
[10] C. A. Lucas, M. Sc. thesis, Universidade Federal do Rio de Janeiro, 1984.
[11] G. G. B. de Souza and C. A. Lucas, in *Abstracts of Contributed Papers, XIV International Conference on the Physics of Electronic and Atomic Collisions, Palo Alto, 1985,* edited by M. J. Coggiola, D. L. Heustis, and R. P. Saxon (North-Holland, Amsterdam, 1985), p. 252.
[12] E. Fainelli, R. Camilloni, G. Petrocelli, and G. Stefani, Nuovo Cimento D **9**, 33 (1987).
[13] A. Szabo and N. S. Ostulund, Chem. Phys. Lett. **17**, 163 (1972).
[14] S. Chung and C. Lin, Phys. Rev. A **8**, 988 (1972).
[15] K. Greenwald and P. W. Langhoff, in *Abstracts of Contributed Papers, XIII International Conference on the Physics of Electronic and Atomic Collisions, Berlin, 1983,* edited by J. Eichler, W. Fritsch, I. V. Hertel, N. Stolterfoht, and U. Ville (ICPEAL, Berlin, 1983), p. 263.
[16] C. E. Bielschowsky, M. A. C. Nascimento, and E. Hollauer, Phys. Rev. A **42**, 5223 (1990).
[17] A. P. Hitchcock, J. Electron Spectrosc. Relat. Phenom. **25**, 245 (1982).
[18] F. Wuilleumier and M. O. Krause (unpublished).
[19] R. B. Kay, Ph. E. van der Leeuw, and M. J. van der Wiel, J. Phys. B **10**, 2513 (1977).
[20] A. Bianconi, H. Peterson, F. C. Brown, and R. Z. Bachrach, Phys. Rev. A **17**, 1907 (1978).
[21] N. Oda, T. Nishimura, and T. Osawa, in *Abstracts of Contributed Papers, XI International Conference on the Physics of Electronic and Atomic Collisions, Kyoto, 1979,* edited by K. Takayanagi and N. Oda (North-Holland, Amsterdam, 1979), p. 408.
[22] R. Camilloni, E. Fainelli, G. Petrocelli, G. Stefani, F. Maracci and R. Platania, in *Wavefunctions and Mechanisms from Electron Scattering Processes,* edited by F. A. Gianturco and G. Stefani, Lecture Notes in Chemistry Vol. 35 (Springer-Verlag, Berlin, 1984), p. 172.
[23] R. Camilloni, E. Fainelli, G. Petrocelli, and G. Stefani, J. Phys. B **20**, 1839 (1987).
[24] J. L. Dehmer and D. Dill, J. Chem. Phys. **65**, 4496 (1976).
[25] T. N. Rescigno and P. W. Langhoff, Chem. Phys. Lett. **51**, 65 (1977). For updated results see T. N. Rescigno and A. Orel, in *Wavefunctions and Mechanisms from Electron Scattering Processes* (Ref. [22]), p. 215.
[26] S. Iwata, N. Kosugi, and O. Nomura, Japan. J. Appl. Phys. **17**, 105 (1978).
[27] T. N. Rescigno and A. E. Orel, J. Chem. Phys. **70**, 3390 (1979).
[28] R. Arneberg, H. Agren, H. Müller, and R. Manne, Chem. Phys. Lett. **91**, 362 (1982).
[29] A. Barth and J. Schirmer, J. Phys. B **18**, 867 (1985).
[30] Theoretical calculation for the GOS distribution of the preionization line in N_2 based on the newly developed generalized multistructural (GMS) model by C. E. Bielschow-

sky, M. A. C. Nascimento, and E. Hollauer, following paper, Phys. Rev. A **45**, 7942 (1992), and references cited therein.

[31] R. S. Barbieri and R. A. Bonham, Phys. Rev. A **44**, 7361 (1991).

[32] See AIP document no. PAPS PLRAA-44-7361-48 for 48 pages of experimental data. Order by PAPS number and journal reference from American Institute of Physics, Physics Auxiliary Publication Service, 335 East 45th Street, New York, NY 10017. The price is $1.50 for each microfiche (60 pages) or $5.00 for photocopies of up to 30 pages, and $0.15 for each additional page over 30 pages. Airmail additional. Make checks payable to the American Institute of Physics.

[33] R. A. Bonham, Chem. Phys. Lett. **18**, 454 (1973).

[34] G. C. King, F. H. Read, and M. Tronc, Chem. Phys. Lett. **52**, 50 (1977).

[35] D. A. Shaw, G. C. King, F. H. Read, and D. Cvejanovic, J. Phys. B **15**, 1785 (1982).

[36] G. R. Wight, C. E. Brion, and M. J. Van der Wiel, J. Electron. Spectrosc. Relat. Phenom. **1**, 457 (1972/73).

[37] A. P. Hitchcock and C. E. Brion, J. Electron. Spectrosc. Relat. Phenom. **18**, 1 (1980).

[38] M. Tronc, G. C. King, and F. H. Read, J. Phys. B **13**, 999 (1980).

[39] C. F. N. Saito and I. H. Suzuki, Phys. Rev. Lett. **61**, 2740 (1988), and references therein.

[40] R. H. J. Jansen, F. J. de Heer, H. J. Luyken, B. van Wingerden, and H. J. Blaauw, J. Phys. B **9**, 185 (1976).

[41] W. Butscher, R. J. Buenker, and S. D. Peyerimhoff, Chem. Phys. Lett. **52**, 618 (1977).

[42] G. R. Wight, M. J. van der Wiel, and C. E. Brion, J. Phys. B **9**, 675 (1976).

[43] B. E. Cole and R. N. Dexter, J. Phys. B **11**, 1011 (1978).

[44] J. A. R. Samson and R. B. Cairns, J. Opt. Soc. Am. **55**, 1035 (1965).

[45] J. E. McGuire, Phys. Rev. **175**, 20 (1968).

[46] Wm. J. Veigele, Atom. Data **5**, 51 (1973).

[47] See Ref. [20] and A. S. Vinogradov, B. Shlarbaum, and T. M. Zimkina, Opt. Spectrosc. **36**, 383 (1974); **36**, 658 (1974).